Supplementary Information

Diiron(II) Pentacarbonyl Complexes as CO-releasing Molecules: Their Synthesis, Characterizations, CO-releasing Behaviours and Biocompatibility

Zhiyin Xiao,[b] Ran Jiang,[a] Jing Jin,[c] Xiuqin Yang,[a] Binyu Xu,[b] and Xiaoming Liu,*[b] Yabing He*[a] and Yi He*[c]

[a] College of Chemistry and Life Sciences, Zhejiang Normal University, Jinhua 321004, China

[b] College of Biological, Chemical Sciences and Engineering, Jiaxing University, Jiaxing 314001, China

[c] Department of Urology, Jiaxing First Hospital, Jiaxing 314001, China

Email: xiaoming.liu@mail.zjxu.edu.cn (X. M. Liu); heyabing@zjnu.cn (Y. B. He); alan1015@21cn.com (Y. He).

Tel./Fax: +86 (0)573 83643937 (X. M. Liu).

Contents

Fig. S14 Mass analysis of the solutions of **1I** (top) and **3Br** (bottom) in DMSO after maintained for 1 h at 37 ^{o}C under an open atmosphere, respectively.

Fig. S15 Mass analysis of the solution of complex **1I** in MeCN (top) or MeOH (bottom) within 5 min.

Fig. S16 Mass analysis of the solution of **3Br** in MeCN within 5 min.

Fig. S17 FTIR spectra of complexes **5** and **6** in DCM.

Fig. S18 Infrared spectral variation during the CO-releasing process of complex **6** (0.0115 mol L^{-1}) in MeCN at 37 ^{o}C an open atmosphere.

Fig. S19 Mass spectrum of the aqueous solution of productions from completed degradation of complex **6**.

Fig. S20 Viabilities of PC-3 cells incubated with the iodo complexes (1I and 2I, a) and bromo complexes (3Br and 4Br, b) at various concentrations for 24 h by standard MTT assays.

Table S1 Selected bond lengths (Å) and angles (°) for complexes **3Br** and **4Br**.

Table S2 Crystal data and structure refinements for complexes **5** and **6**.

Table S3 Selected bond lengths (Å) and angles (°) for complexes **5** and **6**.

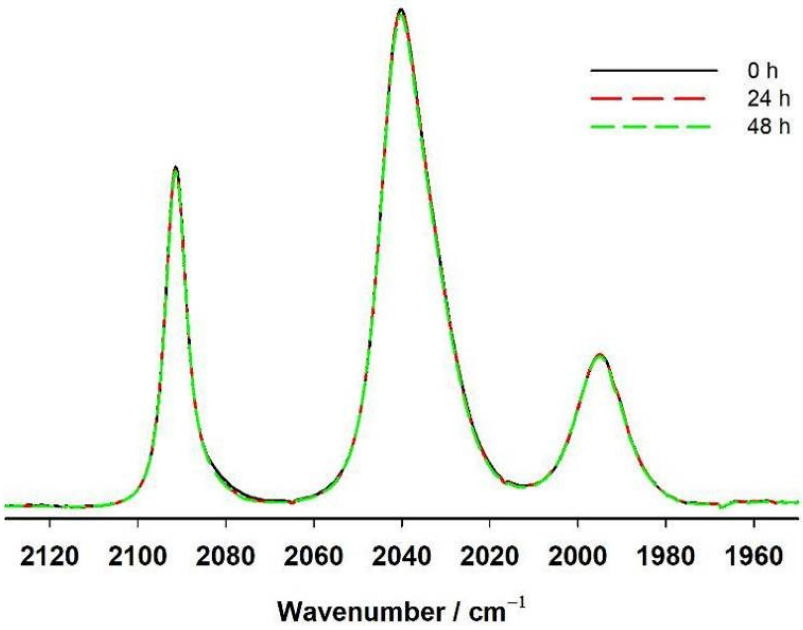

Fig. S1 FTIR spectra of **3Br** which were solidly maintained under an open atmosphere in daylight at ambient temperature for 0 h, 24 h and 48 h and then dissolved in DCM, respectively.

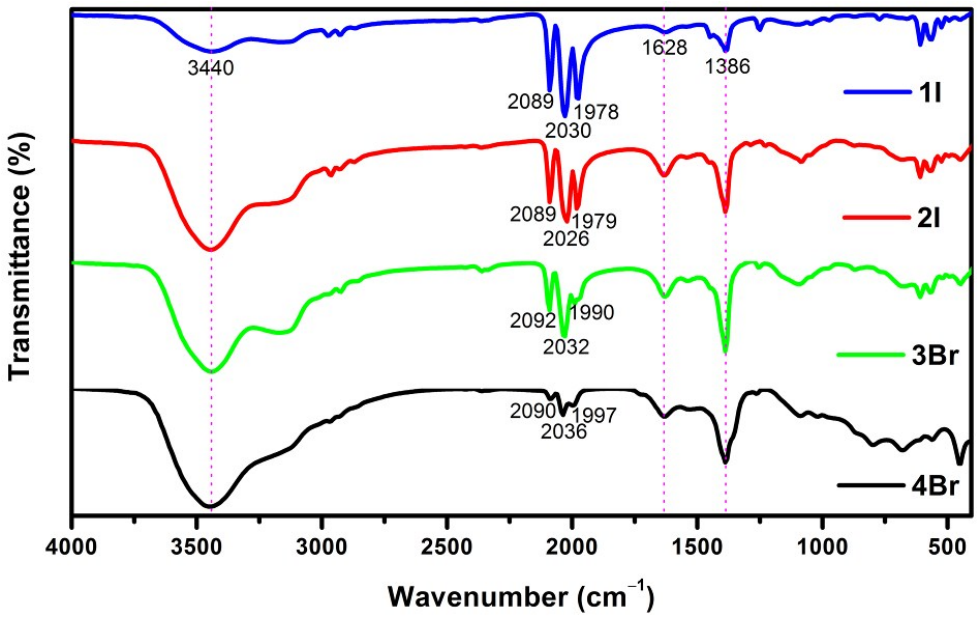

Fig. S2 FTIR spectra of **1I**, **2I**, **3Br** and **4Br** in KBr pellets.

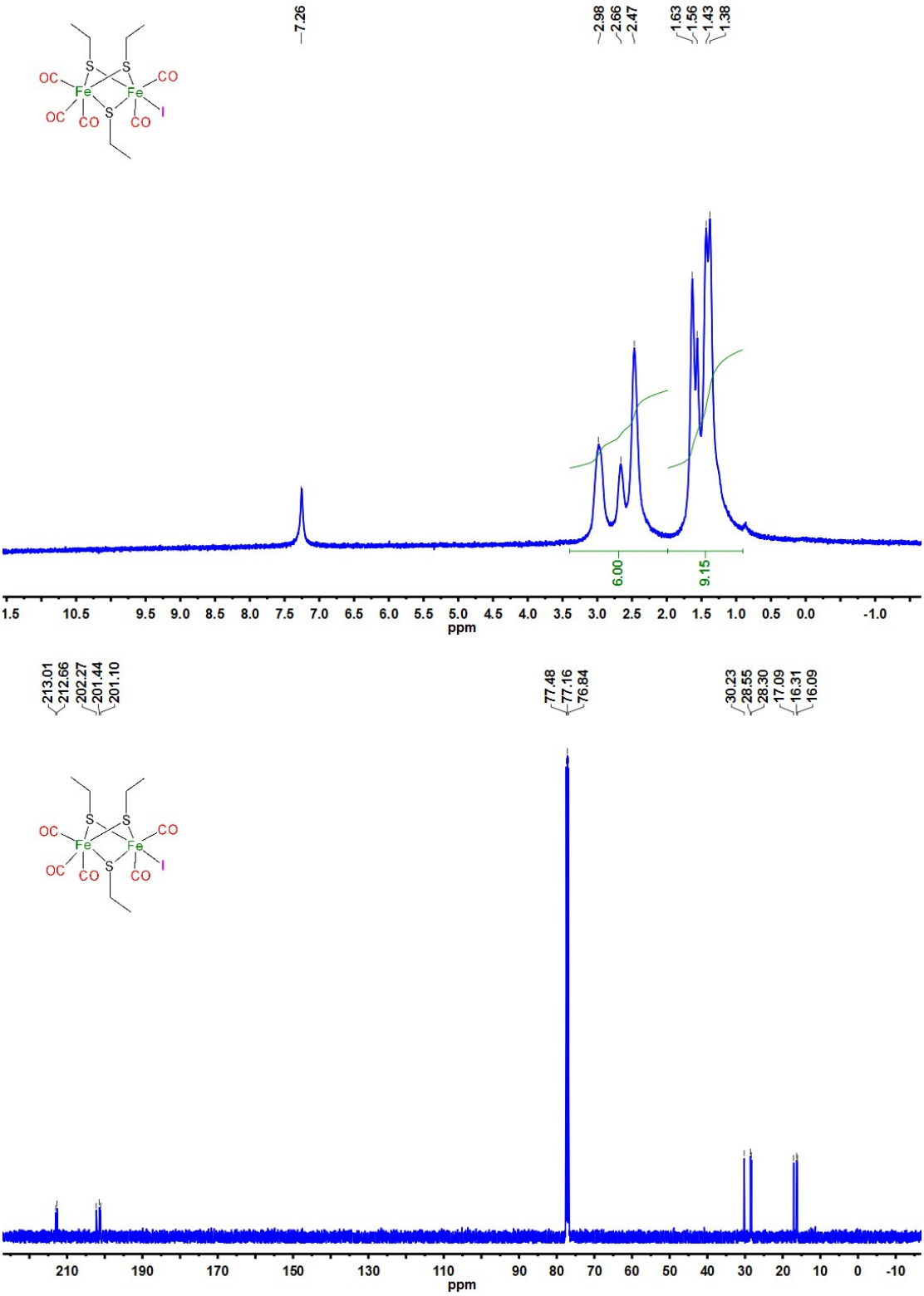

Fig. S3 ^{1}H / ^{13}C NMR spectra of complex **1I** in $CDCl_3$ at room temperature.

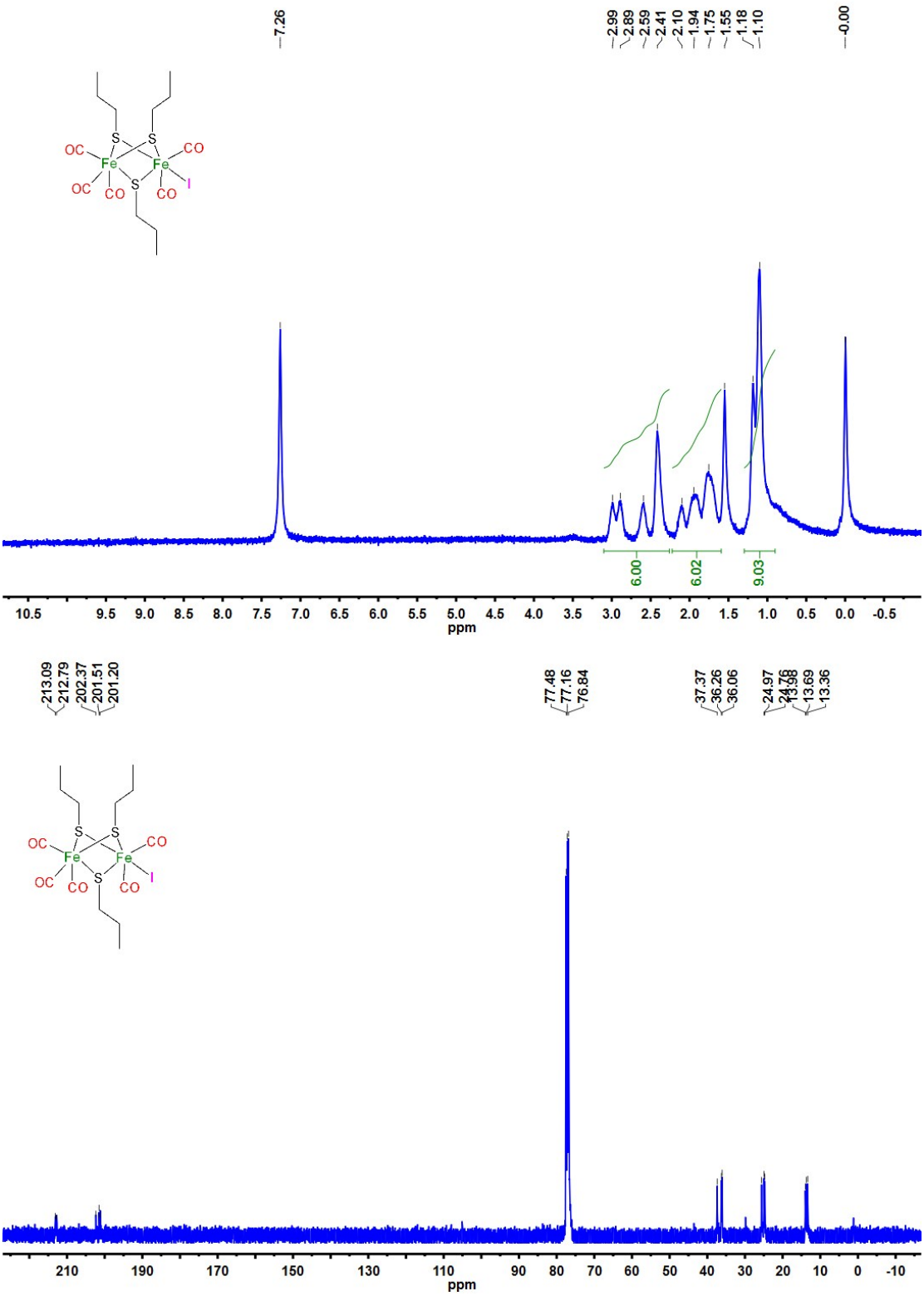

Fig. S4 ^{1}H / ^{13}C NMR spectra of complex **2I** in $CDCl_3$ at room temperature.

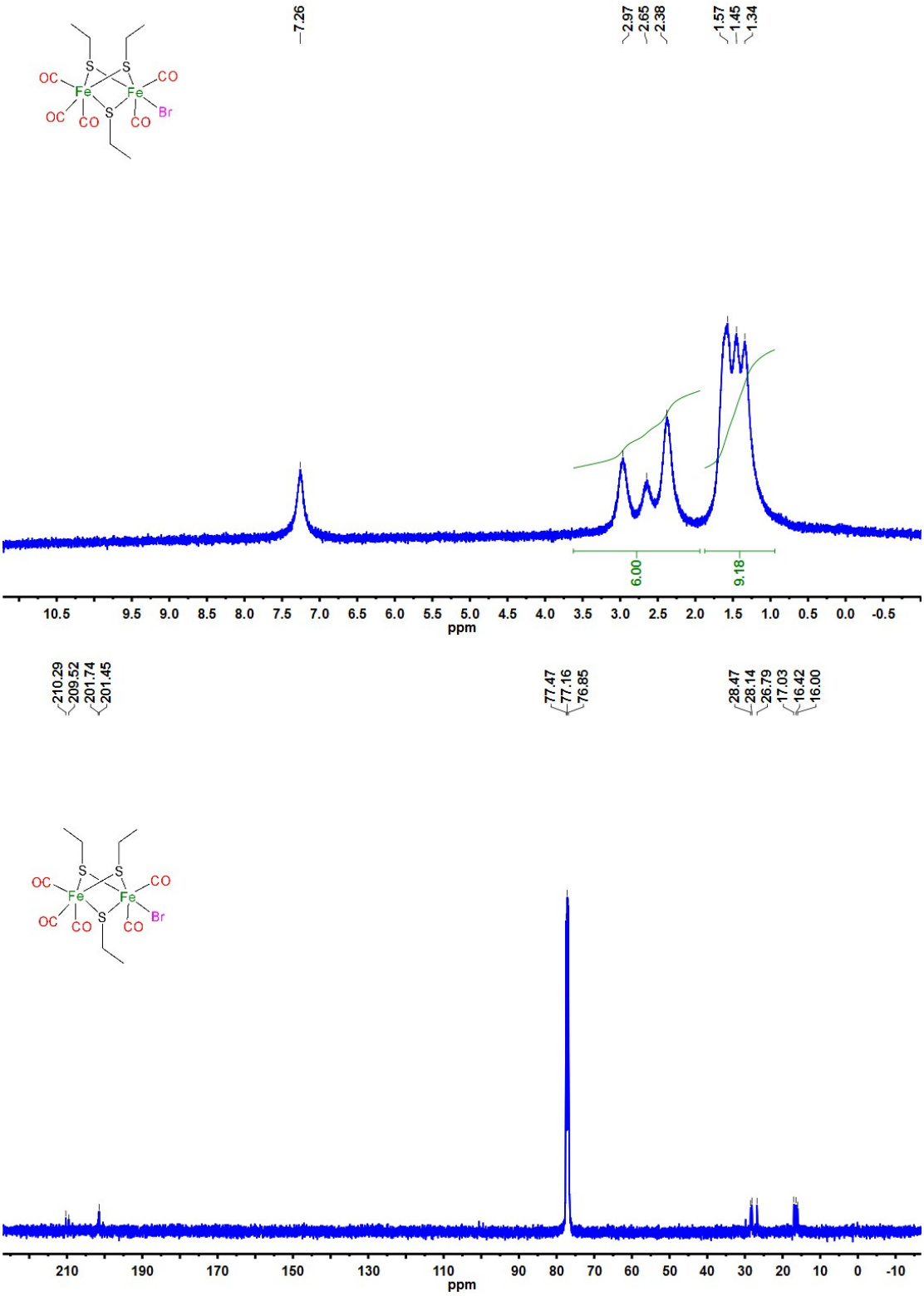

Fig. S5 ^{1}H / ^{13}C NMR spectra of complex **3Br** in $CDCl_3$ at room temperature.

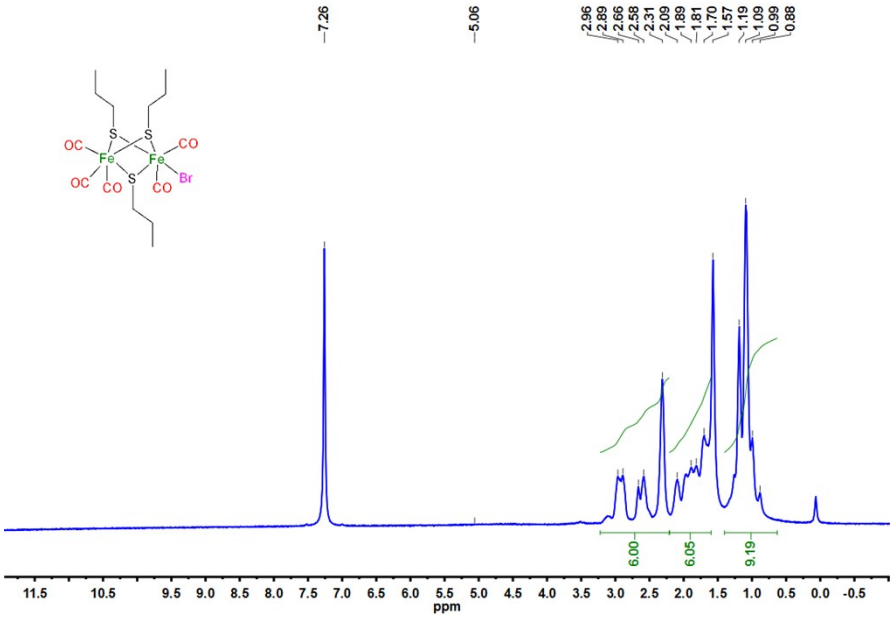

Fig. S6 ^{1}H NMR spectra of complex **4Br** in $CDCl_3$ at room temperature.

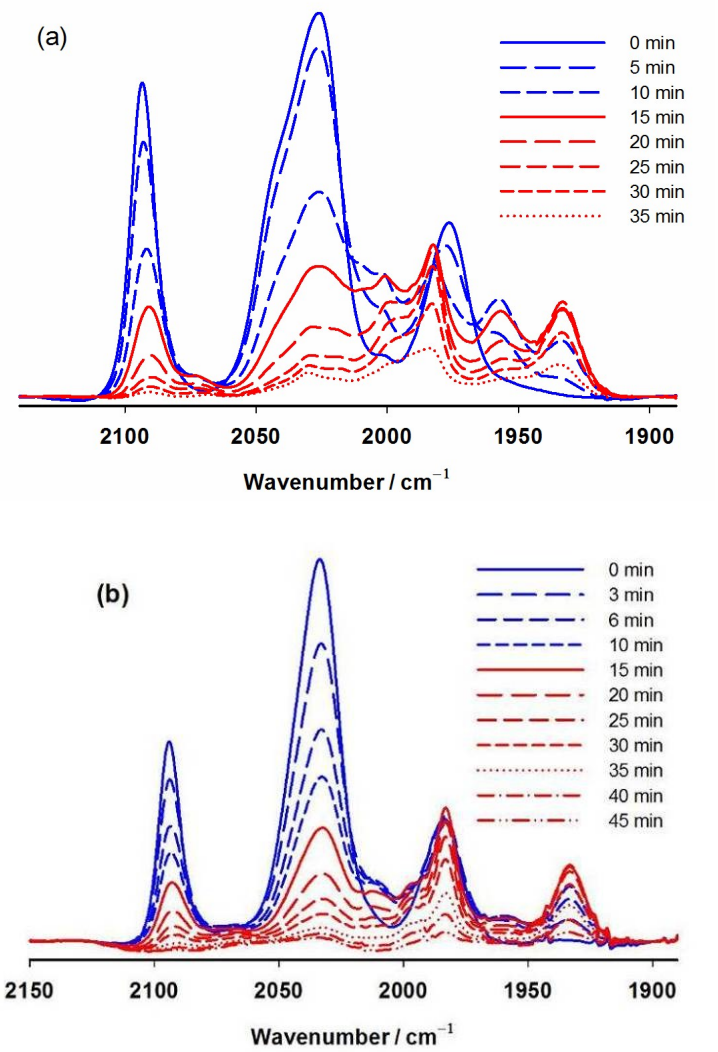

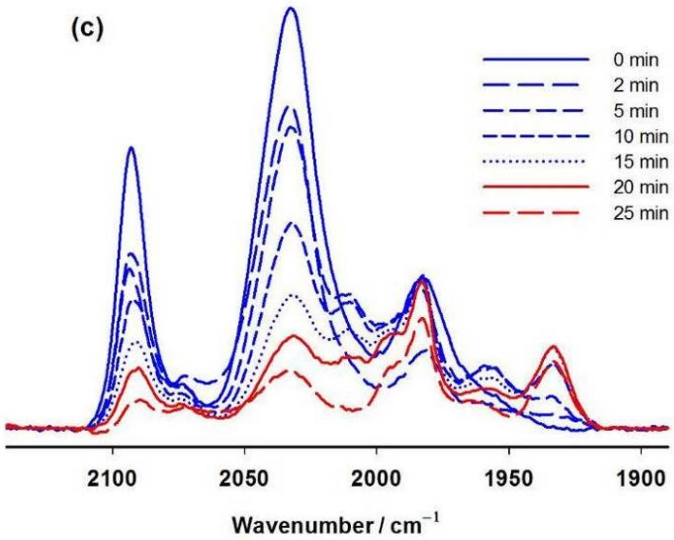

Fig. S7 Infrared spectral variation during the CO-releasing process of complexes **2I** (a), **3Br** (b) and **4Br** (c) in DMSO with a concentration of 0.0115 mol L^{-1} at 37 ^{o}C under an open atmosphere in dark, respectively.

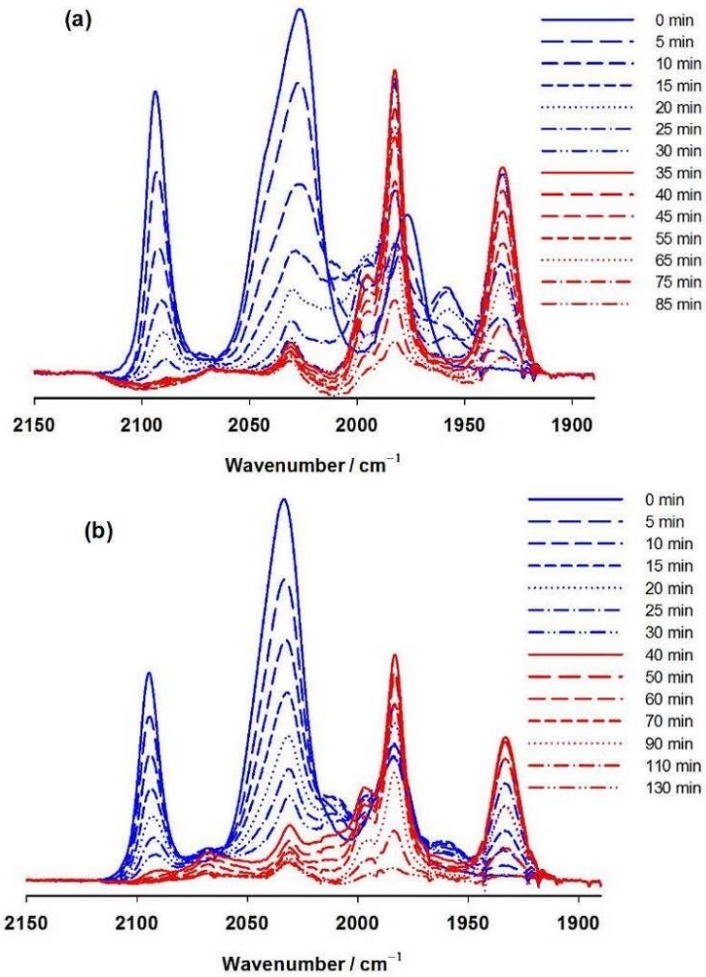

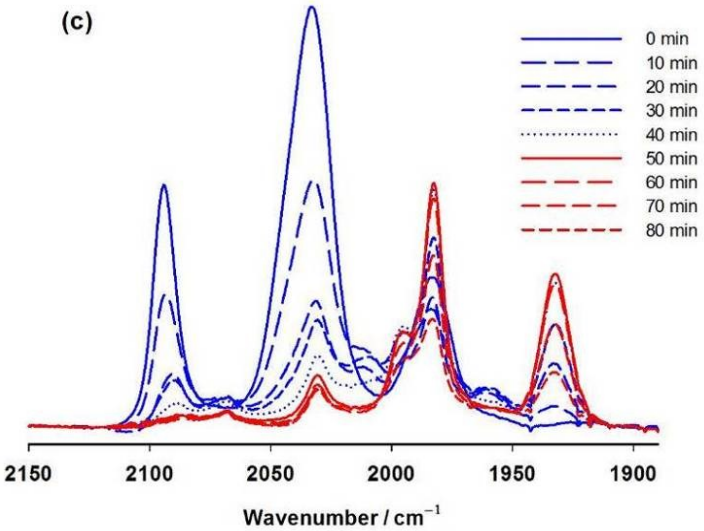

Fig. S8 Infrared spectral variation during the CO-releasing process of complexes **2I** (a), **3Br** (b) and **4Br** (c) in DMSO with a concentration of 0.0115 mol L^{-1} at 37 ^{o}C under an anaerobic atmosphere in dark, respectively.

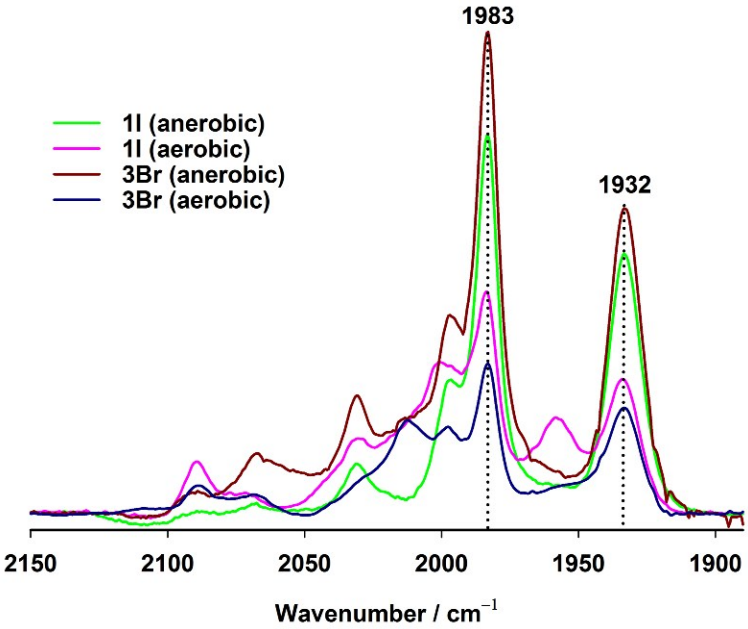

Fig. S9 FTIR spectra during the CO-releasing process of anaerobic **1I** (green), aerobic **1I** (pink), anaerobic **3Br** (brown) and aerobic **3Br** (blue), when the reaction proceeded in DMSO for 40 min at 37 ^{o}C in dark.

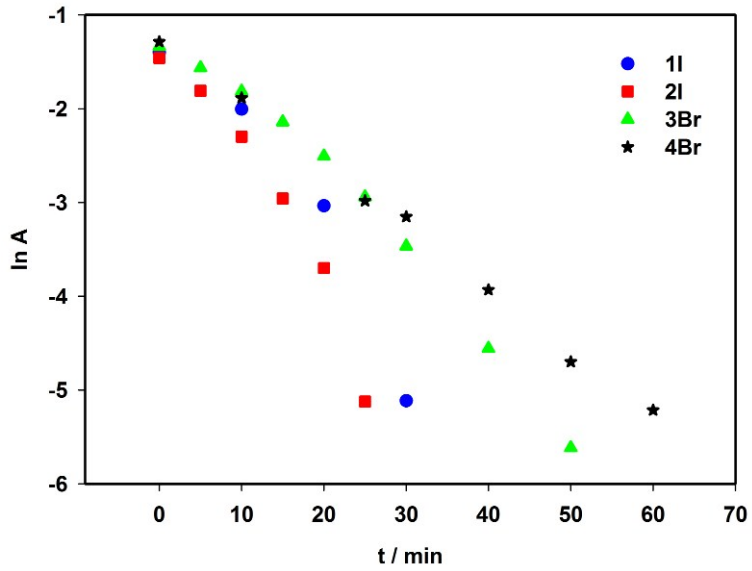

Fig. S10 Plots of the absorbance of complexes **1I**, **2I**, **3Br** and **4Br** (at 2093 cm^{-1}) against the time in an anaerobic DMSO at 37 °C in dark.

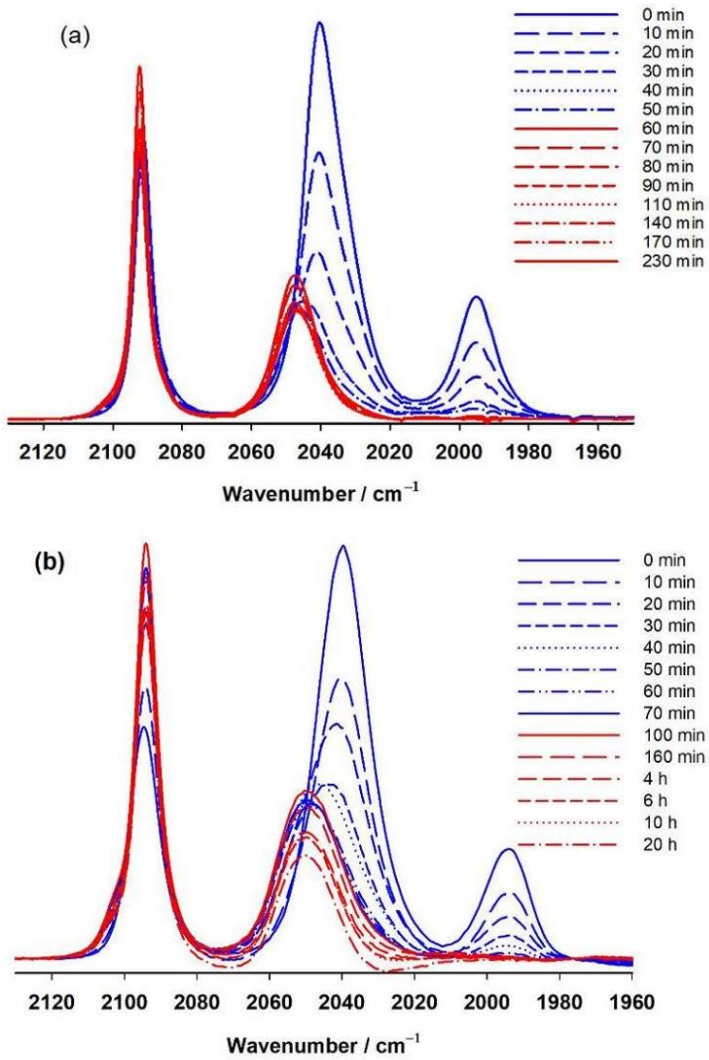

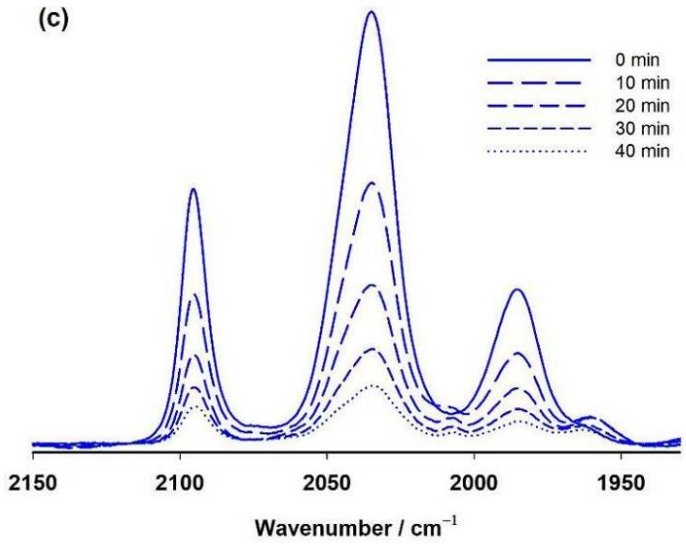

Fig. S11 Infrared spectral variation during the CO-releasing process of **3Br** (0.0115 mol L^{-1}) in DCM (a), MeOH (b) and DMF (c) at 37 ^{o}C under an open atmosphere, respectively.

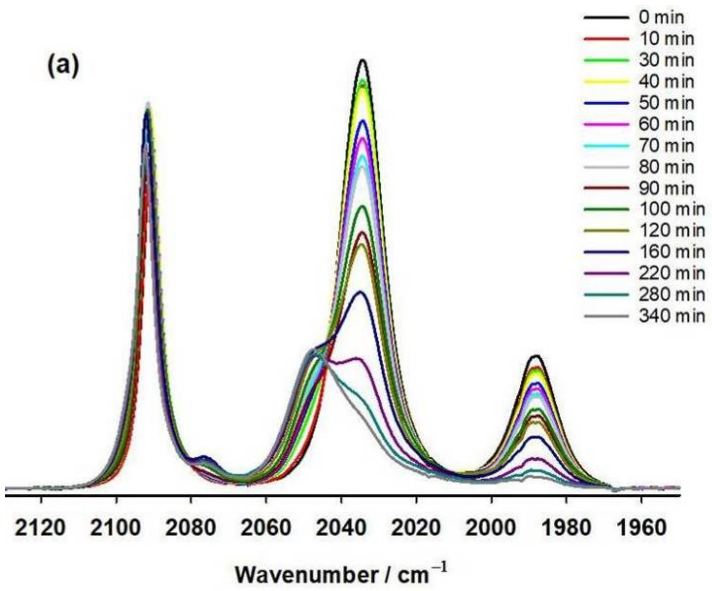

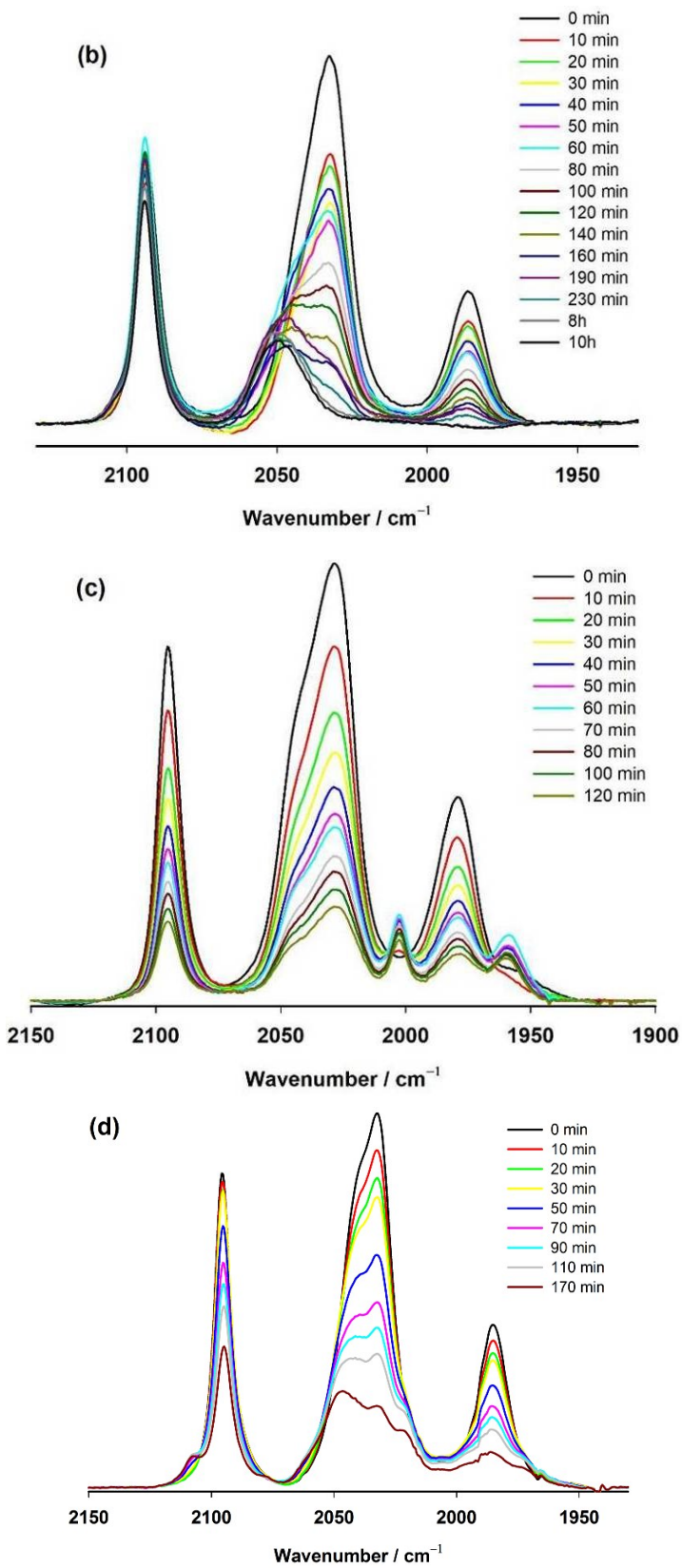

Fig. S12 Infrared spectral variation during the CO-releasing process of **1I** (0.0115 mol L^{-1}) in DCM (a), MeOH (b), DMF (c) and MeCN (d) at 37 ^{o}C under an open atmosphere, respectively.

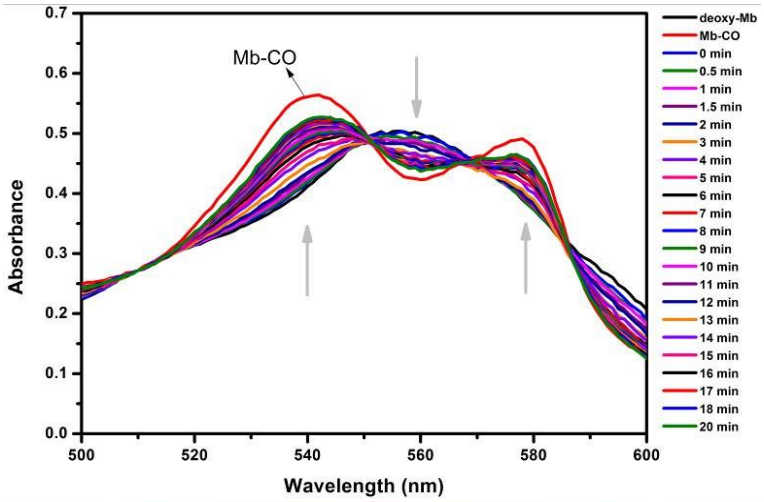

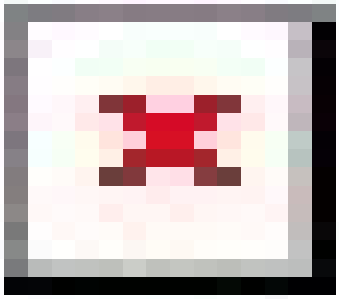

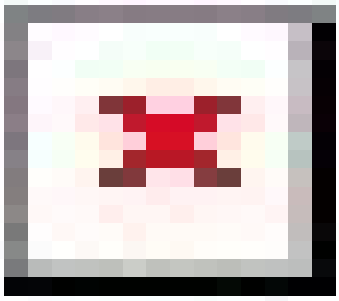

Fig. S13 (Top) Spectra of deoxy-Mb and Mb-CO, respectively and spectral variations along the CO-releasing process; (Middle) The variation of the concentration of [Mb-CO] derived from the differential absorbance (ΔA) at 540 nm with time coordinate;

(Bottom) Plots of the natural logarithm of [Mb-CO] (μmol L^{-1}) against time. Linear fittings were performed at the first three minutes and the last thirteen minutes. First-order reaction model fitting for the stages were performed with a K_{obs} of 0.49 and 0.03 min^{-1}, respectively. The two stages are probably attributed to the decomposition of the parent diiron(II) complex **1I** and the intermediate.

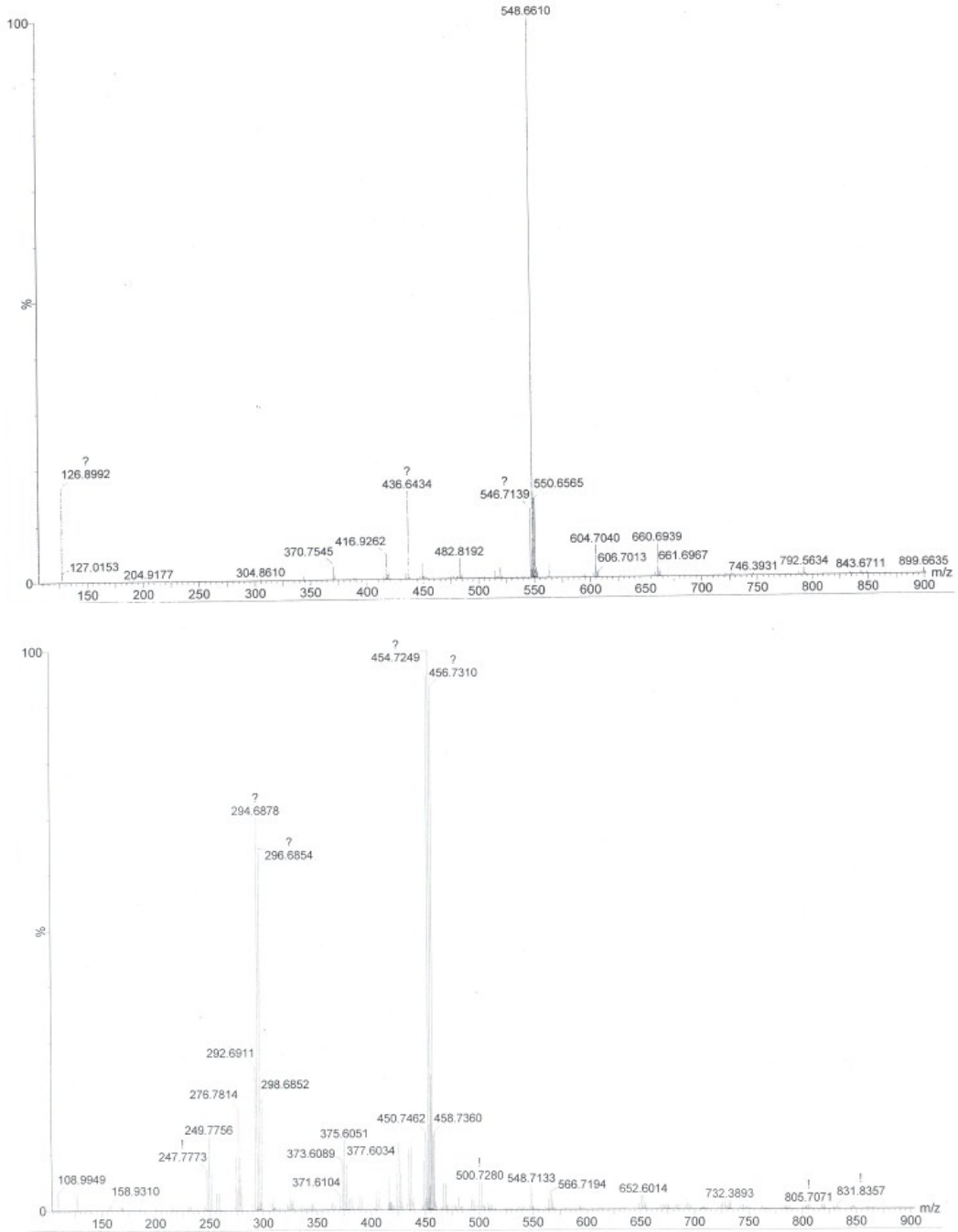

Fig. S14 Mass spectra of complexes **1I** (top) and **3Br** (bottom) in DMSO after being maintained for 1 h at 37 °C under open atmosphere, respectively.

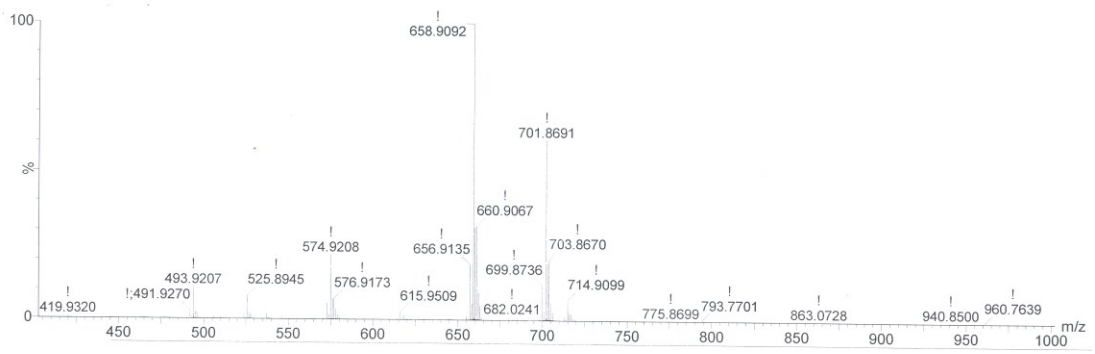

Fig. S15 Mass spectrum of complex **1I** in MeCN (top) or MeOH (bottom) within 5 min.

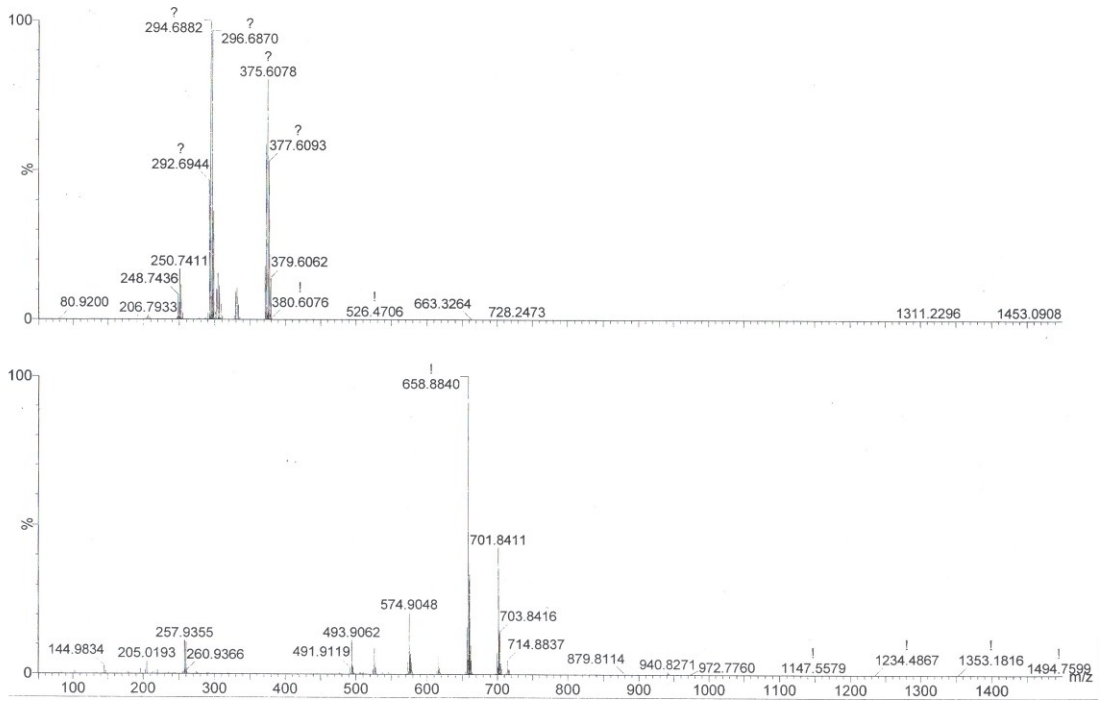

Fig. S16 Mass spectra of complexe **3Br** in MeCN within 5 min.

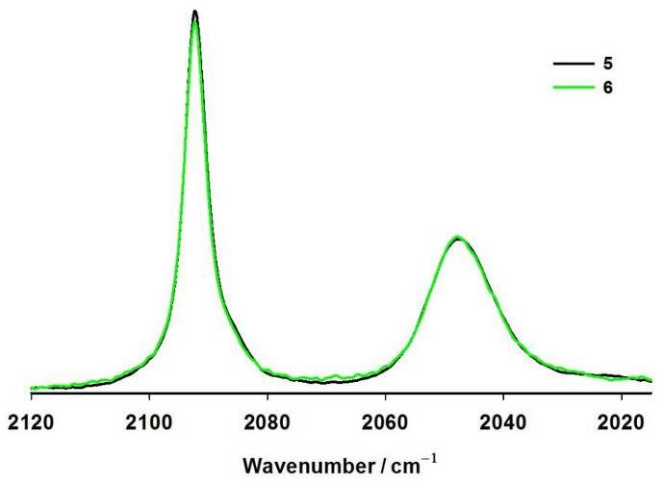

Fig. S17 FTIR spectra of complexes **5** and **6** in DCM.

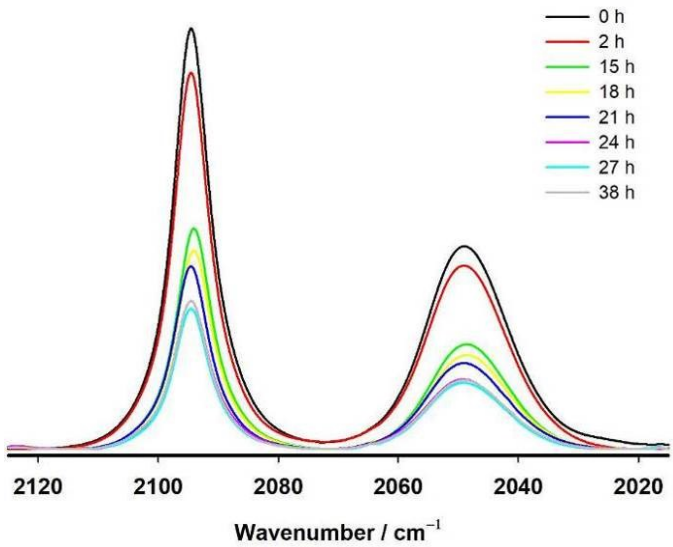

Fig. S18 Infrared spectral variation during the CO-releasing process of complex **6** (0.0115 mol L^{-1}) in MeCN at 37 ^{o}C an open atmosphere.

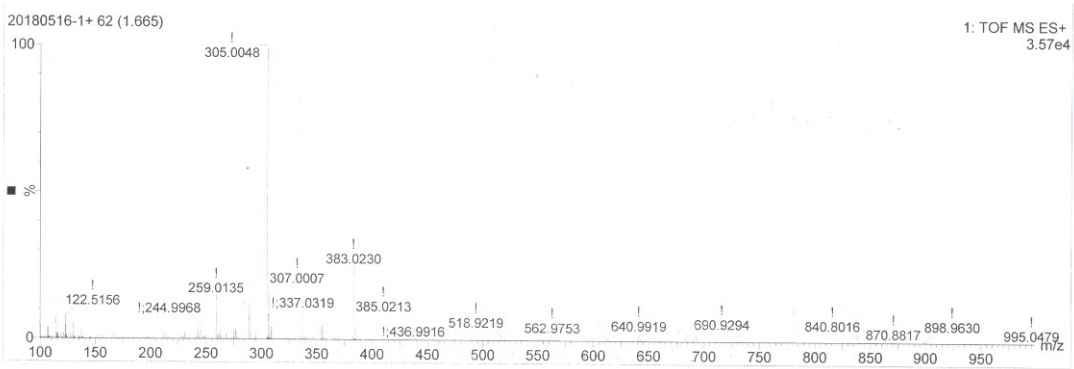

Fig. S19 Mass spectrum of the aqueous solution of productions from completed degradation of complex **6**.

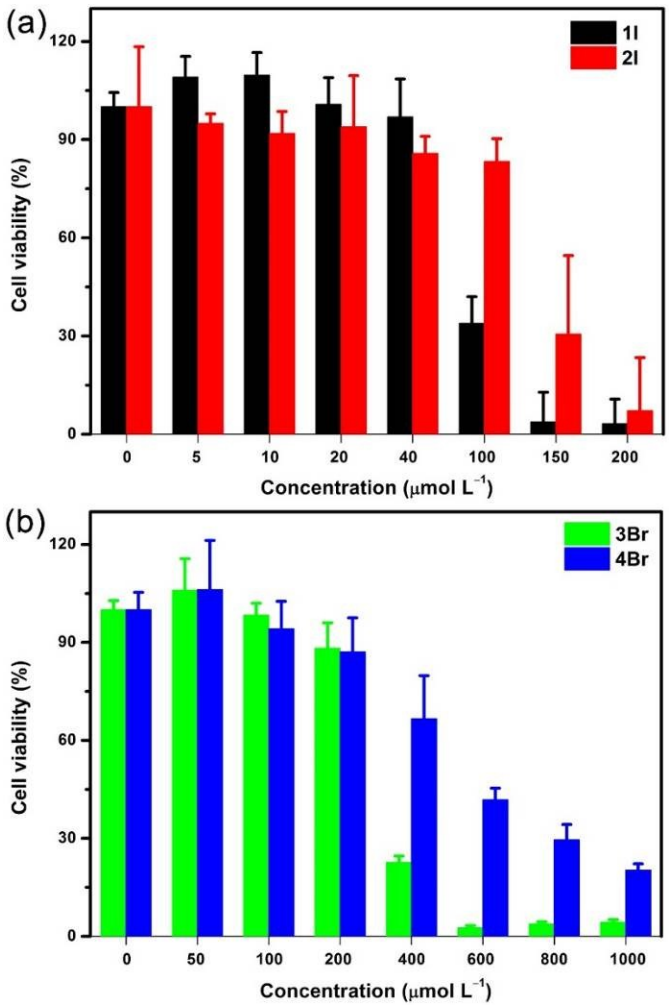

Fig. S20 Viabilities of PC-3 cells incubated with the iodo complexes (1I and 2I, a) and bromo complexes (3Br and 4Br, b) at various concentrations for 24 h by standard MTT assays.

Table S1 Selected bond lengths (Å) and angles (°) for complexes **3Br** and **4Br**.

3Br		**4Br**	
Fe(1)-Fe(2)	3.052	Fe(1)-Fe(2)	3.073
Fe(1)-Br(1)	2.444(2)	Fe(1)-Br(1)	2.461(5)
Fe(1)-S(1)	2.259(3)	Fe(1)-S(1)	2.321(6)
Fe(1)-S(2)	2.337(3)	Fe(1)-S(2)	2.313(6)
Fe(1)-S(3)	2.305(3)	Fe(1)-S(3)	2.287(6)
Fe(2)-S(1)	2.295(3)	Fe(2)-S(1)	2.312(6)
Fe(2)-S(2)	2.314(4)	Fe(2)-S(2)	2.315(6)

Fe(2)-S(3)	2.317(3)	Fe(2)-S(3)	2.302(6)
Fe(1)-C(1)	1.776(13)	Fe(1)-C(1)	1.92(4)
Fe(2)-C(3)	1.839(15)	Fe(2)-C(3)	1.82(3)
Fe(2)-S(1)- Fe(1)	84.15(11)	Fe(2)-S(1)- Fe(1)	83.1(2)
Fe(2)-S(2)- Fe(1)	82.01(10)	Fe(2)-S(2)- Fe(1)	83.2(2)
Fe(2)-S(3)-Fe(1)	82.63(11)	Fe(2)-S(3)- Fe(1)	84.1(2)
S(1)-Fe(1)-S(3)	81.44(12)	S(1)-Fe(1)-S(3)	81.3(2)
S(2)-Fe(1)-S(1)	82.05(12)	S(2)-Fe(1)-S(1)	80.5(2)
S(3)-Fe(1)-S(2)	79.77(12)	S(3)-Fe(1)-S(2)	81.3(2)
S(1)-Fe(2)-S(3)	80.40(12)	S(1)-Fe(2)-S(3)	81.2(2)
S(2)-Fe(2)-S(1)	81.79(12)	S(2)-Fe(2)-S(1)	80.6(2)
S(2)-Fe(1)-Br(1)	97.60(10)	S(2)-Fe(1)-Br(1)	93.6(2)
S(1)-Fe(1)-Br(1)	174.29(11)	S(1)-Fe(1)-Br(1)	97.6(2)
S(3)-Fe(1)-Br(1)	92.88(10)	S(3)-Fe(1)-Br(1)	173.6(2)

Table S2 Crystal data and structure refinements for complexes **5** and **6**.

	5	**6**
CCDC number	1848783	1848782
Empirical formula	$C_{18}H_{30}Fe_3I_3O_6S_6$	$C_{18}H_{30}Fe_4Br_4O_6S_6$
Formula weight	1083.03	1077.78
Crystal system	monoclinic	triclinic
Space group	$P2_1/n$	P-1
a/Å	10.7252(4)	9.9734(12)
b/Å	20.1697(6)	11.7281(15)
c/Å	17.0870(6)	17.300(2)
α/°	90	79.277(11)
β/°	106.031(4)	80.459(11)
γ/°	90	65.816(12)

Volume(Å^3)	3552.6(2)	1804.7(4)
Z	4	2
ρcalc (g cm^{-3})	2.025	1.983
F(000)	2076.0	1052.0
Radiation	MoKα (λ = 0.71073)	CuKα (λ = 1.54184)
2θ/°	5.592 to 52.998	9.242 to 144.81
Reflections collected	31586	12142
Independent reflections	7361 (R_{int} = 0.0335)	6949 (R_{int} = 0.2420)
Goodness-of-fit on F^2	1.072	0.902
R_1, wR_2 (I≥2σ(I))	0.0442, 0.0897	0.1188, 0.2233
R_1, wR_2 (all data)	0.0676, 0.0974	0.3573, 0.3574
Max./min. peak (e Å^{-3})	1.36/-1.11	1.10/-0.81

Table S3 Selected bond lengths (Å) and angles (°) for complexes **5** and **6**.

5		**6**	
Fe(1)-Fe(2)	2.9660(9)	Fe (1)-Fe(2)	2.967(4)
I(1)-I(2)	2.9265(6)	Fe(5)-Br(1)	2.339(5)
Fe(1)-S(1)	2.3219(14)	Fe(1)-S(1)	2.323(7)
Fe(1)-S(2)	2.3287(13)	Fe(1)-S(2)	2.296(8)
Fe(1)-S(3)	2.3134(13)	Fe(1)-S(3)	2.295(8)
Fe(2)-S(1)	2.2834(13)	Fe(2)-S(1)	2.267(7)
Fe(2)-S(2)	2.2783(13)	Fe(2)-S(2)	2.298(7)
Fe(2)-S(3)	2.2775(12)	Fe(2)-S(3)	2.302(6)
Fe(1)-C(1)	1.805(6)	Fe(1)-C(1)	1.80(3)
Fe(1)-C(2)	1.813(6)	Fe(1)-C(2)	1.80(3)
Fe(1)-C(3)	1.812(6)	Fe(1)-C(3)	1.92(3)
Fe(2)-S(1)-Fe(1)	80.18(4)	Fe(2)-S(1)-Fe(1)	80.5(2)
Fe(2)-S(2)-Fe(1)	80.15(4)	Fe(2)-S(2)-Fe(1)	80.7(2)

Fe(2)-S(3)-Fe(1)	80.49(4)	Fe(2)-S(3)-Fe(1)	80.3(2)
S(1)-Fe(1)-S(3)	81.95(4)	S(1)-Fe(1)-S(3)	82.5(3)
S(2)-Fe(1)-S(1)	82.06(5)	S(2)-Fe(1)-S(1)	82.0(3)
S(3)-Fe(1)-S(2)	81.99(4)	S(3)-Fe(1)-S(2)	82.4(3)
S(1)-Fe(2)-S(3)	83.58(5)	S(1)-Fe(2)-S(3)	96.5(2)
S(2)-Fe(2)-S(1)	84.02(5)	S(2)-Fe(2)-S(1)	83.4(2)
S(4)-Fe(3)-C(6)	169.73(17)	S(4)-Fe(3)-C(10)	83.6(11)
S(5)-Fe(3)-C(6)	96.24(17)	S(5)-Fe(3)-C(10)	96.7(10)
S(6)-Fe(3)-C(6)	170.21(17)	S(6)-Fe(3)-C(1)	165.9(11)
O(1)-C(1)-Fe(1)	177.6(5)	O(1)-C(1)-Fe(1)	174.8(13)
O(2)-C(2)-Fe(1)	178.8(5)	O(3)-C(3)-Fe(2)	174.5(13)
O(3)-C(3)-Fe(1)	178.3(6)	O(6)-C(6)-Fe(3)	175.0(14)
O(4)-C(4)-Fe(3)	176.6(5)	Br(4)-Fe(5)-Br(1)	109.8(2)
O(5)-C(5)-Fe(3)	178.1(5)	Br(3)-Fe(5)-Br(4)	107.5(2)
O(6)-C(6)-Fe(3)	179.0(5)	Br(3)-Fe(5)-Br(2)	110.9(2)